JTTEE5 16:940–946
DOI: 10.1007/s11666-007-9129-1
1059-9630/$19.00 © ASM International

Peer Reviewed

Evaluation of Strain Field Around Impacted Particles by Applying Electron Moiré Method

Makoto Watanabe, Satoshi Kishimoto, Yongming Xing, Kentaro Shinoda, and Seiji Kuroda

(Submitted March 12, 2007; in revised form September 11, 2007)

Recently, the thermal-spray community has focused considerable attention on cold-spray and warm-spray techniques, in which the temperatures of sprayed particles are kept below their melting point and adhesion occurs based on the impact phenomenon between a solid particle and a substrate. The mechanisms of adhesion are still unclear, but the degree of the mechanical deformation at the interface is considered to be a key factor influencing this mechanism. However, it is very difficult to directly measure the strain at the interface. Instead, in this work, the strain fields on a substrate around an impacted particle sprayed by warm-spray deposition were measured by applying electron Moiré method, and compared with numerical simulation results.

Keywords electron Moiré method, warm spray, particle impact, finite element analysis

1. Introduction

In recent years, cold-spray and warm-spray methods are attracting wide interest from the research community. In these processes, coatings of ductile materials could be produced without significant heating of the sprayed powders, and hence degradation during deposition, such as oxidation can be avoided. Unmelted particles are accelerated to velocities in the order of 500-1200 m/s and impinge on a substrate, where kinetic energy dissipation (Ref 1-9) causes their deformation and bonding.

Therefore, it is essential to understand the impact phenomena between a solid particle and a substrate in order to understand the deposition mechanism. It is generally accepted by various experimental results that there exist a critical velocity, by which the particle velocity has to exceed, in order to cause bonding (Ref 10). Critical velocity depends on sprayed materials and is very important for spray techniques based on the impact of solid particles. Assadi et al. carried out numerical analyses of solid-particle impact behavior for cold-spray process focusing on critical velocity (Ref 11). They calculated the deformation of both the particle and the substrate, together with the resultant strain and temperature distribution as a function of time under adiabatic condition by dynamic analysis. The critical velocity was determined as the velocity at or beyond which adiabatic shear instabilities occur at the interface, and they also demonstrated that the occurrence of shear instabilities correspond to the achievement of maximum local temperature close to the melting point of the particle. In these simulations, many uncertain parameters, such as constants of the constitutive laws of materials for ultra-high deformation rate and thermal-contact resistance has to be assumed (Ref 11, 12). Therefore, the correspondence with real phenomena remains ambiguous, especially for practical spray particle size (25-100 μm). In order to compare with the simulation results, new experimental techniques have to be developed for evaluation of the behavior of a single particle impact.

Electron Moiré method, developed by Kishimoto et al., is a new full-field technique to measure deformations in a microscopic area, which utilizes the changes of Moiré interference fringes due to deformation (Ref 13-15). The Moiré fringes are generated by the interferences of the model grid on the measured surface and the master grid of electron beams in Scanning Electron Microscope (SEM). The range of measurable in-plane deformation can be from 0.1 to 25 μm by applying model grids with different frequency (Ref 14).

Since the deformation caused by an impact of a solid-spray particle appears to be the key factor governing the adhesion of the particle, the present study was motivated to develop a new experimental method to make it possible and to evaluate strain field induced by the particle impact quantitatively. Although deformation fields evaluated by the electron Moiré method are in-plane as shown in Fig. 1, and are not the direct representations of deformations

This article is an invited paper selected from presentations at the 2007 International Thermal Spray Conference and has been expanded from the original presentation. It is simultaneously published in *Global Coating Solutions, Proceedings of the 2007 International Thermal Spray Conference*, Beijing, China, May 14-16, 2007, Basil R. Marple, Margaret M. Hyland, Yuk-Chiu Lau, Chang-Jiu Li, Rogerio S. Lima, and Ghislain Montavon, Ed., ASM International, Materials Park, OH, 2007.

Makoto Watanabe, Satoshi Kishimoto, Kentaro Shinoda, and **Seiji Kuroda**, National Institute for Materials Science, Tsukuba, Ibaraki, Japan; and **Yongming Xing**, Inner Mongolia University of Technology, Hohhot, China. Contact e-mail: WATANABE.makoto@nims.go.jp.

at the interface between a particle and a substrate, it is expected to provide us with some insights regarding the impact behavior.

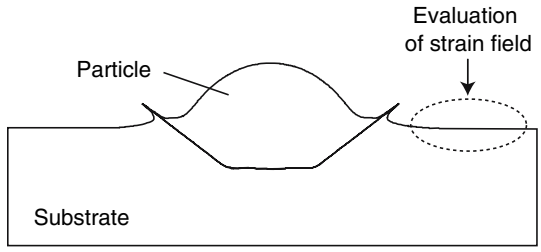

Fig. 1 Schematic of deformation after impact of a solid particle on a substrate. The in-plane strain around the impacted particle indicated by the circle has been evaluated in the current study as the indicator of the deformation amplitude at the interface

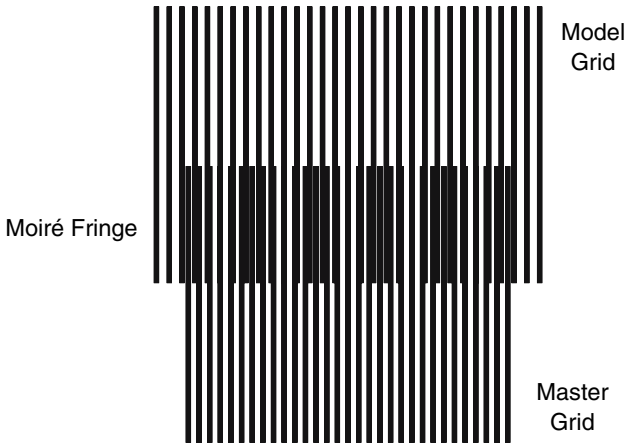

Fig. 2 Concept of Moiré fringes by the interference of the two line grids with different spacing

2. Experiment and Analysis

2.1 Measurement Principle of Electron Moiré Method

Figure 2 shows the general idea of Moiré fringe. The interference of two grids (master and model grids) generates fringes. The width and the space of the fringes depend on the difference of space and vary when the space of the one of the grid is changed. By utilizing this concept, one can measure the deformation of a surface.

In the electron Moiré method, an SEM equipped with a beam-blanking device and a pattern generator for beam control, were employed to produce the master a grid onto sample surface using the primary electron beam. The principle of the electron Moiré method is illustrated in Fig. 3.

A scanning electron beam generate a grid with spacing of a_e (spacing is tailored by the SEM magnification and interval of beam blanking) is exposed on the specimen surface. The specimen surface is deposited with an equally spaced grid lines with spacing a_m as shown in Fig. 3(a). This grid is composed of gold deposited on the specimen surface using a method that is described later. The interference between the specimen grid and the projected electron grid generates electron Moiré fringes of bright and dark lines due to the difference in the contrast of the SEM image formed from the interaction of the specimen surface and the electron beam. Deformation of the specimen causes the variation in the spacing of the model grid, resulting in the variation in the Moiré fringes. For example, when a tensile stress is loaded, the spacing of the grid lines increases from a_m to a'_m and the spacing of Moiré fringes d' becomes shorter (Fig. 3(b)). From the spacing of the Moiré fringes, the tensile strain ε can be expressed by the following equation (Ref 16):

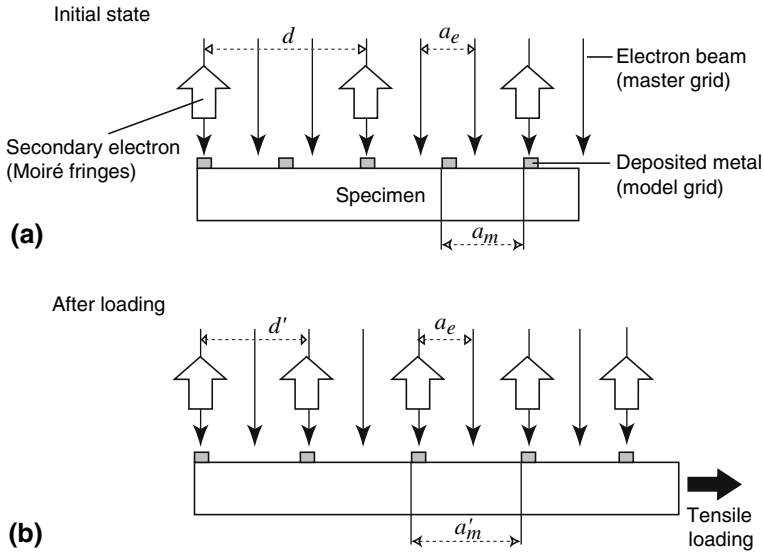

Fig. 3 Schematic illustration of the principle of formation of electron Moiré fringes

$$\varepsilon = \left[\frac{a_e}{d' - a_e}\right] - \left[\frac{a_m - a_e}{a_e}\right]. \quad \text{(Eq 1)}$$

2.2 Development of Model Grid on a Substrate

The model grid on a substrate surface was prepared by electron beam lithography as sketched in Fig. 4 (Ref 16). A polished carbon-steel substrate ($10 \times 10 \times 5$ mm^3) was coated with an electron-sensitive polymer film (EBR-9, Toray Industries Inc., JAPAN) by a spin coating with rotation speed of 2500 rpm for 1 min and then heating at 453 K for 1 h. The thickness of the polymer resist was about 500 nm. The area of about 1 mm^2 on coated surface was exposed to the electron beam in the SEM with controlled beam spacing and the exposed resist was developed. After that, gold was deposited on the surface by ion sputtering to ensure the good visibility in the SEM. Finally, the model grid was obtained by removing the remaining resist by acetone. The example of the prepared lines is shown in Fig. 5. The width of the lines is 1.5 μm and the spacing 2.4 μm. Since a particle can be assumed to be a sphere, the induced strain field could be point symmetrical and hence parallel grids were applied as model grids through the experiment.

2.3 Materials and Spray Conditions

Spherical Copper powders (particle size distribution ranging from 45 to 53 μm) were sprayed onto a grated substrate by warm-spray deposition, which was developed by Kawakita et al. (Ref 4) by modifying High Velocity Oxy-Fuel (HVOF) spray system JP5000 (Praxair, Cincinnati, IN, USA) and has a mixing chamber between a combustion chamber and a powder feed port in order to control the combustion gas temperature with nitrogen gas addition. In this process, the particle temperature could be controlled and sprayed without melting but in higher temperature range compared with a cold-spray deposition. The spray condition is displayed in Table 1. Very fast gun traverse speed (1500 mm/s) and low-powder feed rate (15 g/min) were applied to reduce the number of particles to hit the grated region. Strain around the impinged particles is evaluated from Moiré fringes in the SEM.

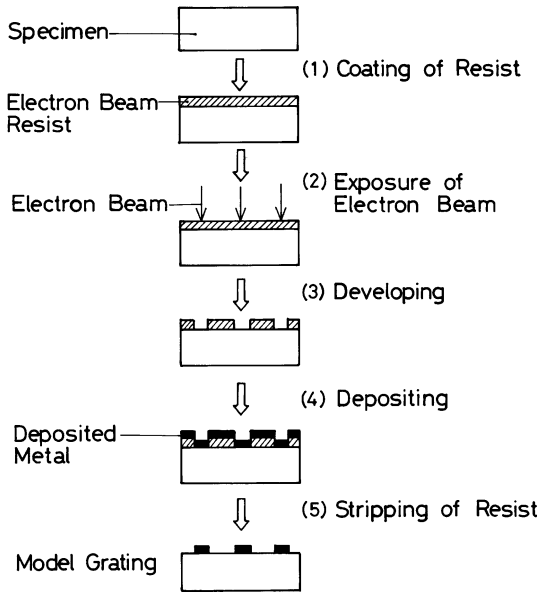

Fig. 4 Flow diagram of the preparation of model grid on a substrate surface by electron beam lithography

2.4 Numerical Analysis

Numerical simulation of the Cu particle impact was carried out, in order to provide rough estimation of the induced strain field following Assadi's model (Ref 11). The analyses were carried out using a commercially available finite element code (ABAQUS version 6.5, ABAQUS Inc., RI, USA). In the model, a Cu particle impacts a carbon-steel substrate at normal angle with given impact velocity and temperature. Axisymmetric model was considered (Fig. 6). The plastic behaviors of the particle and the substrate are assumed to be expressed by Johnson-Cook model, which takes into account the influences of strain hardening, strain rate hardening, and thermal softening (Ref 11, 17). It was assumed that 90% of the plastic strain energy dissipates into heat (Ref 11, 12). Four-node elements with hourglass control were used and the initial element size was 0.2 μm near the contact area for the particle size of 50 μm diameter. The substrate has

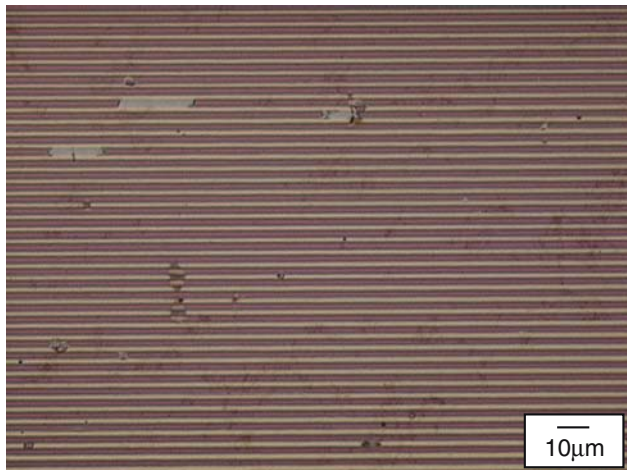

Fig. 5 Model grids on a substrate prepared by electron beam lithography

Table 1 Spray condition of Cu powders with warm-spray equipment

Barrel length, mm	203
Liquid fuel (kerosene) volume flow rate, L min^{-1}	0.35
Primary oxygen volume flow rate, Nm^3 min^{-1}	0.71
Secondary nitrogen volume flow rate, Nm^3 min^{-1}	1.5
Spray distance, mm	180

250×250 μm in the section and the total number of elements were about 20,000. Example of material properties used in the analysis (for room temperature case) was shown in Table 2. In this study, most of the parameters were set as temperature-dependent values based on handbooks (Ref 18, 19). The substrate was fixed at the bottom and horizontal displacement was not allowed at the axis of symmetry. The calculations were done for various particle velocity from 100 to 1000 m/s under the adiabatic condition. The initial temperature of a substrate was assumed to be 293 K, and for particle various initial temperature was calculated from room temperature to 1273 K. These simulation results were compared with the experimental results.

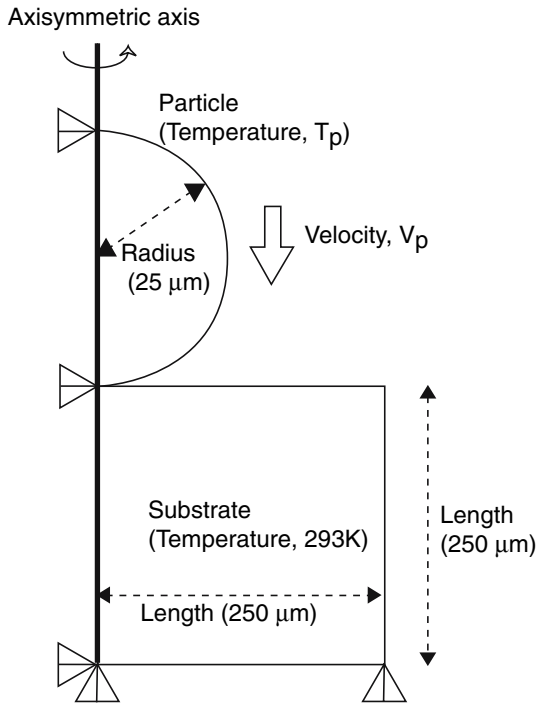

Fig. 6 Schematic of analysis model: a particle (radius r, temperature T_p, velocity V_p) impacting on a substrate

Table 2 Material properties used in the analysis (for room temperature case)

	Unit	Cu	Carbon steel
Density	kg/m^3	8960	7870
Elastic modulus	GPa	124	210
Specific heat	J/(kg K)	383	486
Melting point	K	1356	1538
Thermal-expansion coefficient	10^{-6}/K	16.5	11.6
Yield stress	MPa	90	175
Strain hardening component		0.31	0.39

In this study, most of the parameters were set as temperature-dependent values based on handbooks (Ref 18, 19)

3. Results and Discussions

3.1 Moiré Fringe Around Adhered Particle

Figure 7 shows the Moiré fringe pattern observed around a Cu particle adhered on the substrate. The spacing of the Moiré fringes becomes narrower near the peripheral of the particle while it becomes wider and constant at any place far from the particle. The narrower fringes indicate the occurrence of the in-plane tensile deformation in the y-direction of the picture. The shortening of the spacing can be recognized only at the left side of the particle and cannot be observed at right side implying the non-uniform deformation and hence very likely poor bonding between the particle and substrate. In the present work, only parallel grids were applied under the assumption of point symmetrical deformation but the result is indicating the occurrence of asymmetrical deformations in microscale.

When examining splat morphologies by an optical microscopy or SEM, the ''uniformity of deformation'' cannot be recognized. There are many possible explanations of the origins of this non-uniform deformation, such as (a) impact with oblique angle, (b) anisotropy of the mechanical properties of the polycrystalline substrate, and (c) irregular shape of a particle due to agglomeration with other particles, and so on. Although it is impossible to figure out the reasons in the present study, the Moiré technique could be an appropriate and powerful tool to investigate those factors in future.

3.2 Moiré Fringe Around Imprint

The picture of the Moiré fringe around the imprint of a rebounded particle is shown in Fig. 8. The tendency of the Moiré fringe is similar to the fringe around the adhered particle, but the variation of the spacing is very small along x-axis indicating that a much smaller deformation occurred compared with the adhered case. It is expected

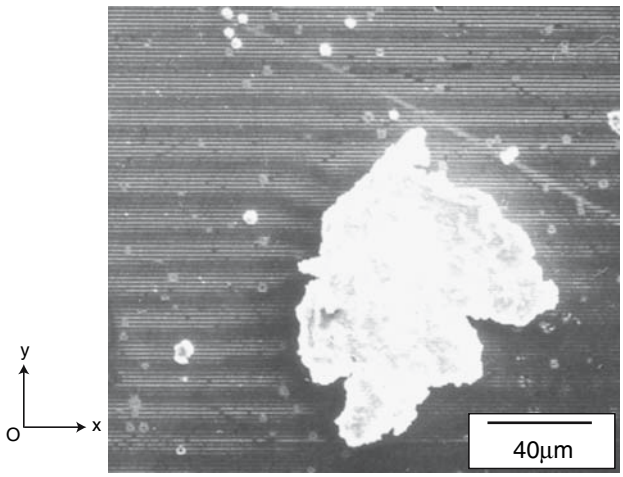

Fig. 7 Moiré pattern observed around the adhered Cu particle sprayed by warm-spray deposition

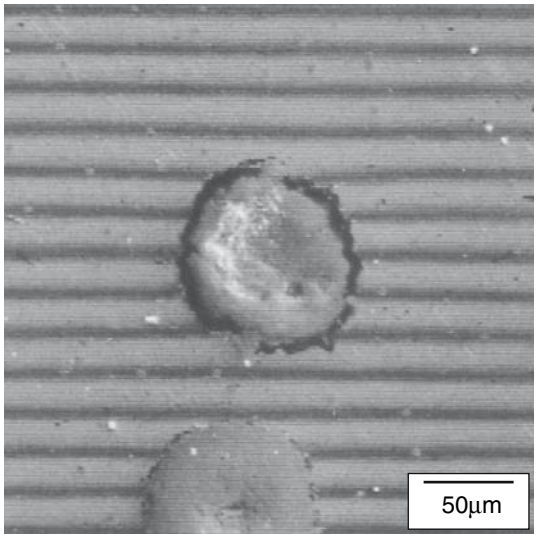

Fig. 8 Moiré pattern around the impression due to the Cu particle impact and rebound without bonding

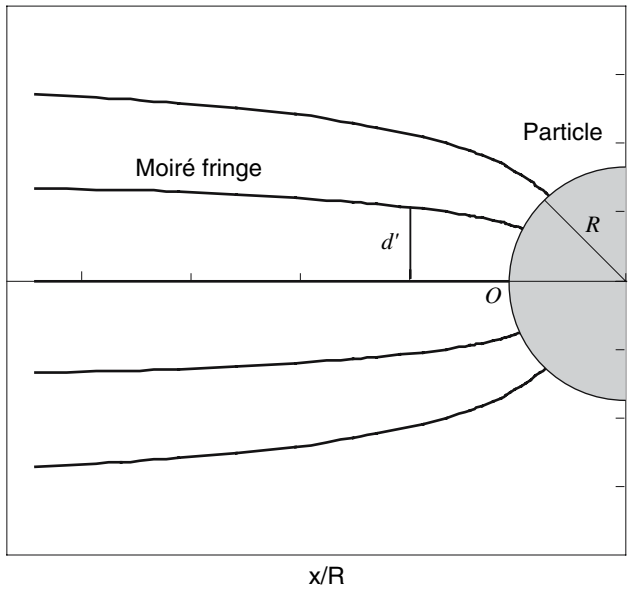

Fig. 9 Schematic to determine the spacing of Moiré fringe along the horizontal axis around a particle

that when large deformation occurs in the substrate surface around the particle, large deformation is also generated at the interface at the same time. Conversely, when the deformation is small on the surface, the deformation at the interface would be also small and the amplitude of the strain would not be enough to satisfy the bonding conditions at the interface. The difference in Moiré fringe patterns displayed in Fig. 7 and 8 is ensuring those general understandings.

3.3 Estimation of Plastic Strain

The tensile strain along the horizontal direction from the particle center was estimated from Eq 1 and the spacing d' (Fig. 9). The obtained values are plotted in Fig. 10 as a function of the distance from the edge of the particle normalized by the radius of a flattened particle R. The solid square and open triangle symbols stand for the strain values of the adhered particle and the imprint of the rebounded particle, respectively. The highest strain values of 5% for the former case and 0.7% for the latter are obtained at the closest point to the particles in both cases.

3.4 Numerical Analysis Results

Figure 11 shows the example of the simulated particle deformation for the particle impact velocity of 500 m/s and the temperature of 773 K. Out flowing of a jet is recognized from the interface between the particle and the substrate and the huge deformation of the particle is manifest. The contour map indicates the distribution of the plastic strain in y-direction. The largest deformation occurs at the interface and as it is far from the interface, the plastic deformation becomes smaller. In order to compare with the current measurement by the electron Moiré technique, the distribution of the plastic strain ε_y along the substrate surface from the particle edge was studied.

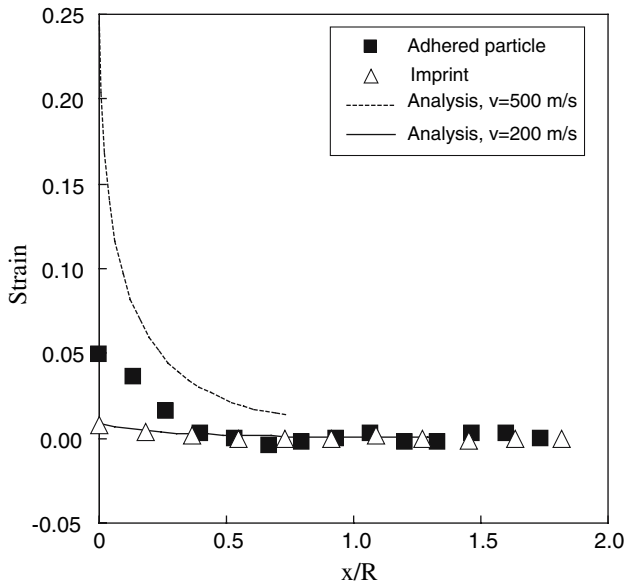

Fig. 10 Evaluated strain variation as a function of the distance from the edge of the particle or the imprint

The numerical analysis results for particle velocity of 200, 500 m/s and temperature 773 K are also plotted in Fig. 10. The dotted line corresponds to the computed velocity of results for a 500 m/s, whereas the solid one stands for a velocity of 200 m/s. First of all, the order of the numerically predicted strain is in the range of 1-20% showing the rather good agreement with the experiment. If a particle uniform temperature of 773 K is assumed, the impact velocity of the adhered particle (Fig. 7) is around

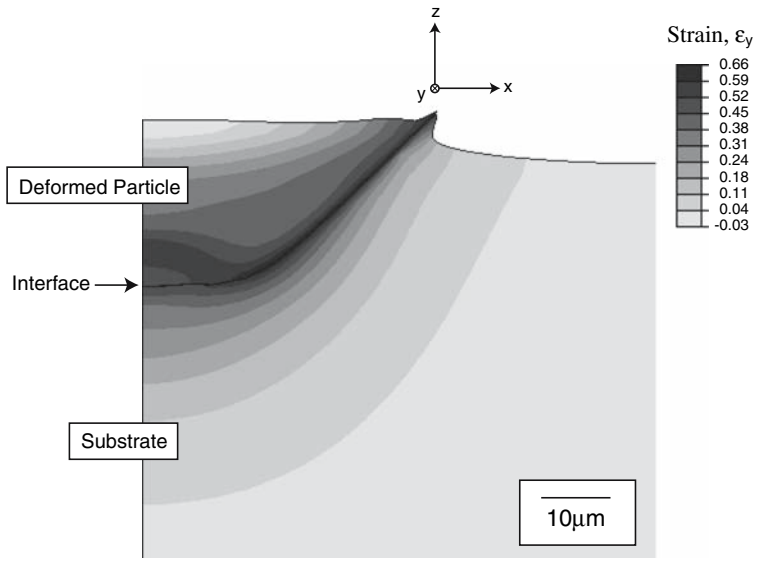

Fig. 11 Distribution of plastic strain ε_y calculated for particle impact velocity 500 m/s and temperature 773 K

300-400 m/s, and about 100-200 m/s for the rebounded case (Fig. 8).

Under the adiabatic condition, the critical velocity of a Cu particle with temperature of 773 K was estimated as about 150 m/s (Ref 20). The predicted critical velocity appears to be in good agreement with the values expected from the present experiment. Kawakita et al. (Ref 21) reported the velocities of Cu particles sprayed by HVOF deposition. The average values were in the range of 400-600 m/s depending on fuel/oxygen ratio indicating good agreement with the current results. Also, Wu et. al. (Ref 22) measured the velocity of the titanium particle, which has an average of 28 μm diameter, deposited by warm spray using DPV 2000 (Tecnar, Canada), and reported 500-800 m/s particle velocity for nitrogen flow rate of 1.5 m^3/min. Copper is twice heavier than titanium and the particle diameter in the present study is 1.75 times larger, the estimated impact velocity of 300-400 m/s seems adequate.

However, the propriety of the assumed particle temperature is difficult to be justified and the temperature will have to be evaluated experimentally. In addition, thermal conduction between a particle and a substrate, which is characterized by thermal contact resistance at the interface, has a large effect on deformation upon impact (Ref 12, 20, 23, 24). Opposite to the adiabatic model, the thermal conduction model will need to be examined in future.

4. Conclusions

The strain field induced by the impact of a solid particle sprayed by warm-spray deposition was quantitatively evaluated applying electron Moiré method. The deformation was tensile in the tangential direction of the particle. The strain values were in the range of 0.7-5% and much larger deformation were recognized around the bonded particle compared with around the imprint of the rebounded particle. It is implied that the strain field evaluation around a particle can be an indicator of bonding state. The evaluated strain values were compared with the numerical simulation. Although the order of the strain shows good agreements and the predicted critical velocity seems adequate, the effect of several parameters such as thermal-contact resistance remains to be clarified in future.

Acknowledgments

M. Watanabe would like to acknowledge financial support by the Iketani Foundation and by the Ministry of Education, Culture, Sports, Science and Technology of the Japanese Government. The authors thank Mr. Komatsu and Mr. Kakeya for supporting deposition of particles.

References

1. S.V. Klinkov, V.F. Kosarev, and M. Rein, Cold Spray Deposition: Significance of Particle Impact Phenomena, *Aerosp. Sci. Technol.*, 2005, **9**(7), p 582-591
2. E. Calla, D.G. McCartney, and P.H. Shipway, Effect of Deposition Conditions on the Properties and Annealing Behavior of Cold-Sprayed Copper, *J. Therm. Spray Technol.*, 2006, **15**(2), p 255-262
3. H.J. Kim, C.H. Lee, and S.Y. Hwang, Superhard Nano Wc-12%Co Coating by Cold Spray Deposition, *Mater. Sci. Eng. A: Struct. Mater. Prop. Microstruct. Process.*, 2005, **391**(1–2), p 243-248
4. J. Kawakita, S. Kuroda, T. Fukushima, H. Katanoda, K. Matsuo, and H. Fukanuma, Dense Titanium Coatings by Modified HVOF Spraying, *Surf. Coat. Technol.*, 2006, **201**(3–4), p 1250-1255
5. T. Marrocco, D.G. McCartney, P.H. Shipway, and A.J. Sturgeon, Production of Titanium Deposits by Cold-Gas Dynamic Spray:

Numerical Modeling and Experimental Characterization, *J. Therm. Spray Technol.*, 2006, **15**(2), p 263-272
6. K. Sakaki and Y. Shimizu, Effect of the Increase in the Entrance Convergent Section Length of the Gun Nozzle on the High-Velocity Oxygen Fuel and Cold Spray Process, *J. Therm. Spray Technol.*, 2001, **10**(3), p 487-496
7. S. Kuroda, Y. Tashiro, H. Yumoto, S. Taira, H. Fukanuma, and S. Tobe, Peening Action and Residual Stresses in High-Velocity Oxygen Fuel Thermal Spraying of 316l Stainless Steel, *J. Therm. Spray Technol.*, 2001, **10**(2), p 367-374
8. S. Kuroda, J. Kawakita, T. Fukushima, and S. Tobe, Importance of the Adhesion of HVOF Sprayed Coatings for Aqueous Corrosion Resistance, *Mater. Trans.*, 2003, **44**(3), p 381-388
9. M. Watanabe, A. Owada, S. Kuroda, and Y. Gotoh, Effect of Wc Size on Interface Fracture Toughness of Wc-Co HVOF Sprayed Coatings, *Surf. Coat. Technol.*, 2006, **201**(3-4), p 619-627
10. C.J. Li, W.Y. Li, and H.L. Liao, Examination of the Critical Velocity for Deposition of Particles in Cold Spraying, *J. Therm. Spray Technol.*, 2006, **15**(2), p 212-222
11. H. Assadi, F. Gärtner, T. Stoltenhoff, and H. Kreye, Bonding Mechanism in Cold Gas Spraying, *Acta Mater.*, 2003, **51**(15), p 4379-4394
12. T. Schmidt, F. Gärtner, H. Assadi, and H. Kreye, Development of a Generalized Parameter Window for Cold Spray Deposition, *Acta Mater.*, 2006, **54**(3), p 729-742
13. S. Kishimoto, M. Egashira, and N. Shinya, Microcreep Deformation Measurements by a Moiré Method Using Electron-Beam Lithography and Electron-Beam Scan, *Opt. Eng.*, 1993, **32**(3), p 522-526
14. S. Kishimoto, H.M. Xie, and N. Shinya, Electron Moiré Method and Its Application to Micro-Deformation Measurement, *Opt. Lasers Eng.*, 2000, **34**(1), p 1-14
15. H.M. Xie, S. Kishimoto, A. Asundi, C.G. Boay, N. Shinya, J. Yu, and B.K.A. Ngoi, In-Plane Deformation Measurement Using the Atomic Force Microscope Moiré Method, *Nanotechnology*, 2000, **11**(1), p 24-29
16. S. Kishimoto, N. Shinya, and M.D. Mathew, Application of Electron Beam Lithography to Study Microcreep Deformation and Grain Boundary Sliding, *J. Mater. Sci.*, 1997, **32**(13), p 3411-3417
17. G.R. Johnson and W.H. Cook, Fracture Characteristics of 3 Metals Subjected to Various Strains, Strain Rates, Temperatures and Pressures, *Eng. Fract. Mech.*, 1985, **21**(1), p 31-48
18. G.R. Johnson, Material Characterization for Warhead Computations, *Prog. Astronaut. Aeronaut.*, 1993, **155**, p 165-197
19. D. Zhao, Hot Tension and Compression Testing, *ASM Handbook*, H. Kuhn and Dana Medlin, Eds., ASM International, 2000, Vol. 8, p 152-163
20. K. Yokoyama, M. Watanabe, S. Kuroda, Y. Gotoh, T. Schmidt, and F. Gärtner, Simulation of Solid Particle Impact Behavior for Spray Processes, *Mater. Trans.*, 2006, **47**(7), p 1697-1702
21. J. Kawakita, K. Isoyama, S. Kuroda, and H. Yumoto, Effects of Deformability of HVOF Sprayed Copper Particles on the Density of Resultant Coatings, *Surf. Coat. Technol.*, 2006, **200**(14-15), p 4414-4423
22. T. Wu, S. Kuroda, J. Kawakita, H. Katanoda, and R. Reed, Processing and Properties of Titanium Coating Produced by Warm Spraying, *Proceedings of the 2006 International Thermal Spray Conference*, 2006
23. K. Shinoda, Y. Kojima, and T. Yoshida, In Situ Measurement System for Deformation and Solidification Phenomena of Yttria-Stabilized Zirconia Droplets Impinging on Quartz Glass Substrate under Plasma-Spraying Conditions, *J. Therm. Spray Technol.*, 2005, **14**(4), p 511-517
24. K. Shinoda, T. Koseki, and T. Yoshida, Influence of Impact Parameters of Zirconia Droplets on Splat Formation and Morphology in Plasma Spraying, *J. Appl. Phys.*, 2006, **100**(7), Art. No. 074903